Reachability of Particle Size Distribution in Semibatch Emulsion Polymerization

Yang Wang and Francis J. Doyle III
Dept. of Chemical Engineering, University of California at Santa Barbara, CA 93106

DOI 10.1002/aic.10225
Published online in Wiley InterScience (www.interscience.wiley.com).

Reachability analysis is critical in the determination of achievable end-point products for complex process systems. In emulsion polymerization, an economically important method of producing various products, particle size distribution (PSD) is an important property of the latex produced. However, the population balance modeling framework does not yield direct solutions to reachability analysis for the resulting nonlinear distributed systems. In this article, a programming-based approach is introduced for the reachability analysis of the final PSD for general particulate systems described by population balance models. In the application to a semibatch styrene homopolymerization system, the reachable region is defined for both the nominal and perturbed cases, with final PSDs characterized as multi-Gaussian distributions. Sensitivity studies reveal the limiting factors in determining the achievable final products, and quantitative criteria are developed. The evolution of the reachable region in the case of midcourse correction reveals the difficulties encountered during in-batch control, and shows the best control performance achievable given the limited on-line measurements. © 2004 American Institute of Chemical Engineers *AIChE J,* 50: 3049–3059, 2004
Keywords: particle size distribution control, population balance model, reachability, nonlinear programming, emulsion polymerization

Introduction

Emulsion polymerization is a multiphase reaction system in which the main reacting components are in the dispersed organic phase. The amphiphilic surfactant molecules are used to stabilize the dispersed phases. Polymerization is initiated in the aqueous phase by water-soluble (ionic) initiators. The oligomers formed in the aqueous phase nucleate new particles either by entering into micelles, which are aggregates of surfactant molecules (micellar nucleation), or by precipitating out of the aqueous phase (homogeneous nucleation). The polymer chains inside the particle propagate at very high rates compared to that in the aqueous phase, causing the particles to grow in size. The growth dynamics depend on the number of polymer chains within the particles. Particles can also increase in size by coalescence with other particles, either because of insufficient stabilization by surfactants or because of the shear stress imparted on the particles by the mixing in the reactor.[1,2] The economic value of emulsion polymerization is dependent on the production of high-quality polymers, where the particle size distribution (PSD) is essential to determine the quality of end-point products such as its rheological properties, adhesion, drying characteristics, and film-forming properties. These depend on the entire PSD rather than the average properties indicated by a small number of moments. Therefore, the control of the entire PSD as an end-objective in emulsion polymerization is well motivated in industrial practice (see, for example, the recent review by Congalidis and Richards[3]). Distribution control is also facilitated by recent advancements in measurement techniques and computational approaches.[4].

The various applications of the emulsions target different PSDs, usually complex and multi-modal. For example, the PSD is typically characterized by the means and variances of each mode, or sometimes upper and lower particle sizes. On the

Correspondence concerning this article should be addressed to F. J. Doyle III at doyle@engineering.ucsb.edu.

other hand, the classes of distributions that can be potentially produced might be limited, depending not only on the polymer system, but also on the process constraints and on the initial conditions. It is therefore imperative to identify the classes of PSDs that are potentially reachable (that is, can be produced by current particulate process and admissible operating conditions). In addition to the assessment of achievable end-point product, reachability analysis plays an important role in the design of in-batch control algorithms because of the irreversible system dynamics. For example, one critical question is whether the original targeted PSD is rectifiable in the presence of initial disturbances, and whether it will remain rectifiable after significant delays in sampling and measuring the intermediate distribution.

There is a rich literature on modeling emulsion polymerization processes. In contrast, there have been relatively few analysis results published for the control of PSD (notably Daotidis and Henson,[5] Flores-Cerrillo and MacGregor,[6] Liotta et al.,[7] Ma et al.,[8] and Semino and Ray[9,10]) where its evolution is described by population balance models. On the mathematical modeling side, the population balance describes the behavior of the entire population (such as the PSD) by modeling the average phenomena of the individual particle. The Reynolds transport theorem is used to derive conservation equations in continuum mechanics, which is supplemented with initial and boundary conditions. Therefore, it accounts for the events of particle nucleation and breakage, particle growth attributed to polymerization, and particle growth attributed to coagulation. Typical population balance models are represented by partial differential equations (PDEs) in the particle properties and time. The particle properties include both the internal coordinates, such as particle size, and external coordinates, such as the physical location. In most cases, the population balance models are also complemented by differential and algebraic equations (DAEs) to address the dynamics of the environmental conditions (continuous phase variables[11]). The solution methods for population balance models have been reviewed in several papers.[12–14]

From the perspective of reachability analysis, the complexity of the underlying mathematical framework [PDE system or even its discretized version in terms of ordinary differential equations (ODEs)] precludes a rigorous mathematical analysis. Many theoretical efforts in the literature have emphasized the exact controllability and stabilizability for linear hyperbolic and parabolic PDE systems,[15,16] which are unrealistic approximations of the particulate systems considered in this work. Two notable exceptions are the work of Liotta et al.[7] and Semino and Ray.[9,10] In the former, a lumped dynamic model was developed for the diameter ratio of a bimodal distribution, and the reachable region for this controlled property was determined using sensitivity to key kinetic and physical parameters. The latter work considers the controllability of emulsion systems in both the constrained and unconstrained cases. A key insight obtained there is that the controllability properties of the reactor are strongly influenced by both constraints on the manipulated variables and by the structure of the controller [such as proportional integral (PI) vs. proportional-integral-derivative (PID)]. However, the assumption of particle age as the only internal coordinate (so as to yield a closed-form analytical solution) excludes its application to most realistic particulate systems. From the perspective of optimization-based approaches, Crowley et al.[17] addressed the computation of surfactant feed profiles for matching a PSD to a prespecified target in the batch emulsion polymerization of styrene. Although the polymerization was limited to short reaction times (interval I), at least in batch/semibatch emulsion polymerization processes, this is the first successful simulation attempt at matching a full PSD to a target distribution. Solving the nontrivial recipe optimization problem using sequential quadratic programming (SQP) has been found to be an efficient tool to assess the influence of different objective function norms and key operating conditions.

In the current work, a systematic reachability study of PSDs has been performed using recipe optimization. The test bed in this work is a styrene semibatch emulsion homopolymerization system, described by a "zero–one" model.[18] A definition of ε-reachability is introduced for a general particulate system based on an equivalent recipe optimization problem. This is followed by a parametric characterization of the targeted final PSDs as multi-Gaussian distributions. The subsequent section discusses the reachable regimes for both unimodal and bimodal distributions, as well as the influence of initial conditions, control vector parameterization (CVP), and batch time. Next, sensitivity studies reveal the limiting factors in determining the achievable final products, and quantitative criteria are developed. Finally, the evolution of the reachable region in the face of disturbances and uncertainties is discussed. The reachability analysis in the case of midcourse correction reveals the difficulties encountered during in-batch control, corresponding to the best achievable control performance given the limited online measurements.

Reachability of the Particulate System

Emulsion polymerization is representative of the class of particulate systems described by population balance equations, which also include crystallization, precipitation, and granulation. The system is modeled by the evolution of the distribution of number of particles per unit volume, $n(r, t)$. It is assumed in this work that particle size r is the only internal coordinate (that is, the location in property space).

Zero–one emulsion polymerization system

The so-called *zero–one model* is a multidistribution population balance model based on the assumption that the rate of radical–radical bimolecular termination within a latex particle is very fast relative to the rate of radical entry into the particles.[1] As a result, latex particles contain either zero or one radical at a given instant.

In brief, the particle size population is divided into a population containing zero radical, $n_0(r)$, and a population containing one radical, $n_1(r)$. The one-radical population is further divided into a population containing a polymer radical, $n_1^p(r)$, which would not readily diffuse out of the particle because of its size, and a population containing a monomer radical formed from chain transfer reaction, $n_1^m(r)$, which can readily exit the particles. The balance equations for these populations in a semibatch reactor are given by

$$\frac{\partial n_0(r)}{\partial t} = \rho(r)[n_1^p(r) + n_1^m(r) - n_0(r)] + k_0(r)n_1^m(r) \quad (1)$$

$$\frac{\partial n_1^p(r)}{\partial t} = \rho_{init}(r)n_0(r) - [\rho(r) + k_{tr}C_p]n_1^p(r) + k_pC_pn_1^m(r)$$

$$- \frac{\partial}{\partial r}[G(r)n_1^p(r)] + \sum_{i=z}^{j_{crit}-1} k_{em,i}[Micelle][IM_i]\delta(r - r_{nuc}) \quad (2)$$

$$n_1^m(r) = \frac{k_{e,E}[E]n_0(r) + k_{tr}C_pn_1^p}{\rho(r) + k_{pe}C_p + k_0(r)} \quad (3)$$

$$n(r) = n_1^p(r) + n_1^m(r) + n_0(r) \quad (4)$$

where the volumetric particle growth rate is given by

$$G(r) = \frac{k_pC_pw_m}{4\pi r^2\rho_PN_A} \quad (5)$$

Here, the quasi-steady-state assumption is applied to $n_1^m(r)$ to derive an algebraic expression for this population; $\rho(r)$ represents an overall radical entry rate into particles; $k_0(r)$ is the radical exit rate; ρ_{init} is the entry rate of initiator derived polymer radicals only (no monomer radicals); k_p is the propagation rate constant; C_p is the monomer concentration in polymer particles; and $\delta(r - r_{nuc})$ in the expression for n_1^p denotes that nucleation of particles occurs at a minimum size, r_{nuc}.

The interaction and conversion between the two populations of different identities precludes the use of the method of characteristics to obtain a closed-form solution. In this case, the PDEs are discretized using orthogonal collocation on finite elements (OCFE) to yield ODEs. Within each of the 12 finite elements chosen over the particle size domain, the solution is approximated using a 5th-order Lagrange interpolant polynomial. Further details of the model and numerical solution techniques are described in Crowley et al.[17] and Coen et al.[18]

Generally, the "zero–one" kinetics focuses on the early stage of emulsion polymerization (interval I in Crowley et al.[17]) where particle size is small and particles are rich in monomer. Unlike the later regimes (intervals II and III) dominated by particle growth, the system incorporates current theory on particle nucleation, particle growth resulting from propagation, and growth resulting from coagulation. Because of the relatively high surfactant concentrations and the low solids concentration, coalescence is assumed to be negligible in this study. We have studied coagulation in other polymer systems.[19] However, this study focused on a simple system to highlight the effectiveness of the programming-based reachability analysis, and attempted to draw connections to the physio-chemical phenomena of polymer growth and nucleation. Meanwhile, the process example still reflects many of the complexities that make the control of PSD a very difficult and practical problem. It is also consistent with the control practice of minimizing, instead of manipulating, the coalescence phenomenon in this stage of polymerization.

Reachability of final PSD

For a general dynamic system, given fixed values of the initial time t_0, and the terminal time t_f, a reachable region is defined as the envelope in state space, $x(t_f)$, that can be reached from suitable initial conditions, $x(t_0)$, through the use of admissible control.[7,20] However, the absence of a general approach to obtain closed-form solutions has precluded the possibility of a rigorous analysis of reachability for the population balance systems. For instance, the multiple distributions and interactions based on statistical reaction mechanisms do not admit closed-form solutions by the method of characteristics. There is no way to trace a deterministic growth path for any individual particle.

In the context of the current work, reachability is defined in an equivalent, programming-based manner, as the existence of a feasible solution to a recipe optimization problem to reach the targeted final PSD at specified time t_f. However, the exact reachability condition is difficult to ascertain for practical PSD control problems, given the inherent limitations, such as the reaction mechanism, and the uncertainties in determining the target PSD. Also, to account for external limitations such as model mismatch, parameter uncertainties, inconsistent measurement, as well as the inaccurate control vector parameterization, the concept of *ε-reachability* is introduced here.

Using control vector parameterization, the recipe optimization problem is formulated to minimize the sum of the squared deviation between the targeted final PSD, $n^{target}(r)$, and that predicted by the model, $n^{model}(r, t_f)$, as follows

$$\min_u J_1 = \frac{\sum_k [n^{model}(r_k, t_f) - n^{target}(r_k)]^2}{n_{scale}} \quad (6)$$

where u denotes the parameterized control vector. n_{scale} is a standardization factor given by

$$n_{scale} = \sum_k [n^{target}(r_k)]^2 \quad (7)$$

Definition. *Given a threshold value ε, the targeted final PSD is defined to be ε-reachable if the optimized objective function J_1 satisfies*

$$J_1 \leq \varepsilon \quad (8)$$

For this specified styrene emulsion homopolymerization system, surfactant and initiator feed rates are chosen as the manipulated variables. When solving the above recipe optimization problem, each of the input profiles is discretized as 10 equally spaced heaviside functions, with the amplitudes of the piecewise constant control actions as decision variables. The reagent feed rates are set to zero during the last 20 min of the operation to avoid the formation of very small particles. At first, the batch time t_f has been fixed at 2 h (120 min). However, as shown in the results, the reachability of the final PSD will be strongly affected by the length of the batch time.

The formulated dynamics optimization problem is solved by using the sequential quadratic programming algorithm FSQP.[21] It is well known that a gradient-based nonlinear programming will guarantee the convergence only to a local optimum. However, for the styrene polymerization problem considered in this work, it has been verified that the local optimum obtained is quite close to the global optimum. A cross-validation procedure is used to minimize the influence of local optima in the following reachability analysis.

Unless specified otherwise, the reachability results presented hereafter refer to the ε-reachability, rather than the exact reachability. A value of $\varepsilon = 0.05$ is used to specify an acceptable neighborhood around the original target. Certainly the measurement noise and the normal variability of the process play important roles when determining ε for a real process. However, the current simulation study focused on the influence of the reaction mechanism itself, and draws on the authors' experience with an experimental emulsion reactor. No additional statistical variations have been considered in the model.

Parametric characterization of final PSD

For visualization purposes, the targeted final PSDs need to be characterized in a finite dimensional parametric space. Observations from industry have indicated that many measured PSDs could be well approximated by combination of a few Gaussian or log-normal distributions, which could be attributed to the inherent mechanism of the capillary hydrodynamic fractionator (CHDF). Given that the unimodal and bimodal distributions are the most interesting cases in application, the final PSDs (for the coagulation-free cases) are described by multi-Gaussian distributions. In the case of two basis functions, this is represented as follows

$$n^{target}(r, p) = k_1\exp[-(r - a_1)^2/\sigma_1^2] + k_2\exp[-(r - a_2)^2/\sigma_2^2] \tag{9}$$

where the parameters $p = \{a_i, k_i, \sigma_i \mid i = 1, 2\}$ are the mean radii, amplitudes, and variances for primary and secondary modes, respectively. All the final PSDs are subject to a fixed solids concentrations at the terminal time, which is described by an equality constraint

$$\int_{r_{nuc}}^{r_{max}} r^3 n^{target}(r, p)dr = constant \tag{10}$$

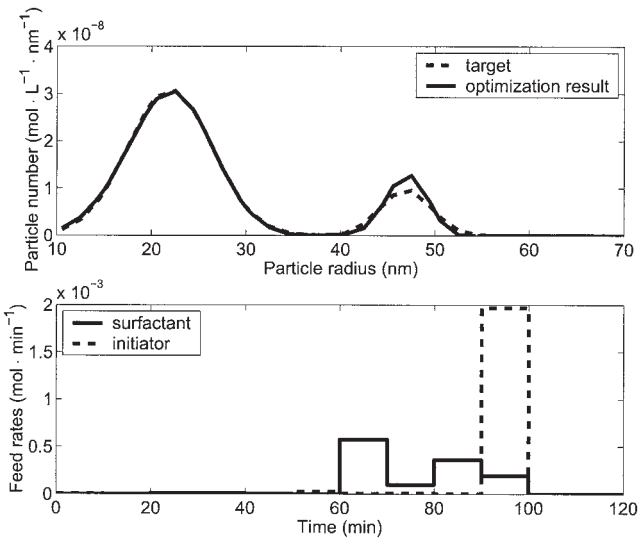

Figure 1. Recipe optimization results with predetermined initial conditions.

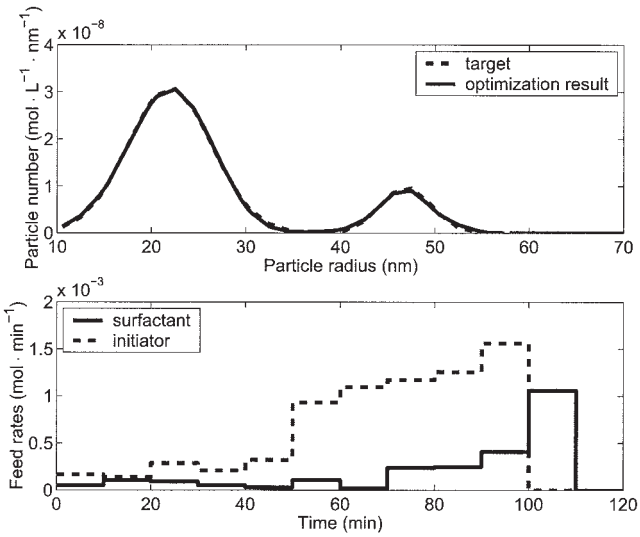

Figure 2. Recipe optimization results with initial condition $S(t_0)$ optimized.

This generates a fair basis of comparison on PSD reachability for different operating conditions.

Results for Nominal System

Effect of the initial reaction conditions

A nominal bimodal distribution is set as the targeted final PSD in the recipe optimization problem (dashed line in Figure 1). In the first formulation, the initial molar number of surfactant $S(t_0)$ is predetermined as 2.5×10^{-3} mol. Given the later input profiles as decision variables, the recipe optimization result (solid line in Figure 1) shows that the number density of the primary mode (large particle size) is always larger than the targeted value, whereas the secondary mode (small particle size) remains well reachable. Consequently, the entire distribution is not reachable.

Detailed simulation results suggest that the monomer droplets exist throughout the batch operation (that is, there is always sufficient monomer within the reactor). Given the particle growth model (Eq. 5) for a "zero–one" system, the volumetric particle growth rate becomes essentially size independent. Because coagulation is presumed negligible, the unreachable mode must be caused by the limited nucleation rate. In this case, the homogeneous nucleation rate is negligible compared with the micellar nucleation rate, which indicates that the surfactant mole number is the limiting state variable.

An analysis of the solution reveals that, at early times, the optimized surfactant input is at its lower bound of 0, which suggests that the lack of reachability is caused by a high initial surfactant mole number, $S(t_0)$. As a result, $S(t_0)$ is included in the decision variables in an extended formulation, which leads to the attainment of the targeted final PSD (Figure 2), with a smaller $S(t_0) = 1.51 \times 10^{-3}$ mol. In summary, the influence of initial conditions may be critical and is not always rectifiable by later inputs because of the irreversibility inherent in the process. Because the total amounts of surfactant feed remain comparable between the two optimization results, it also suggests that not only the amount, but also the timing, of input

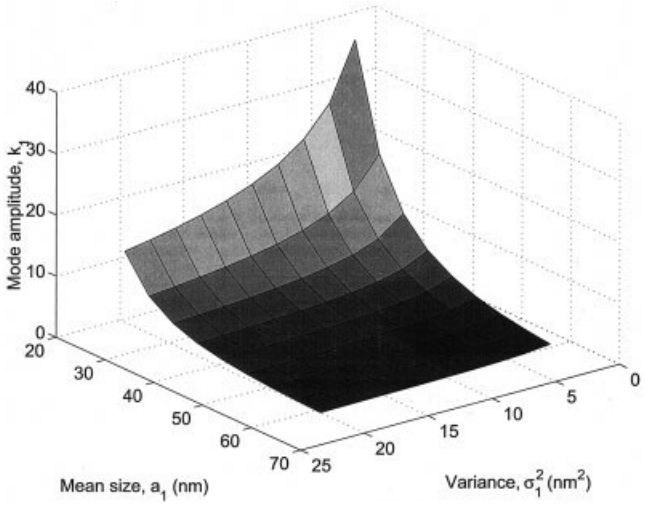

Figure 3. Map of parameter k_1 for all candidate PSDs.

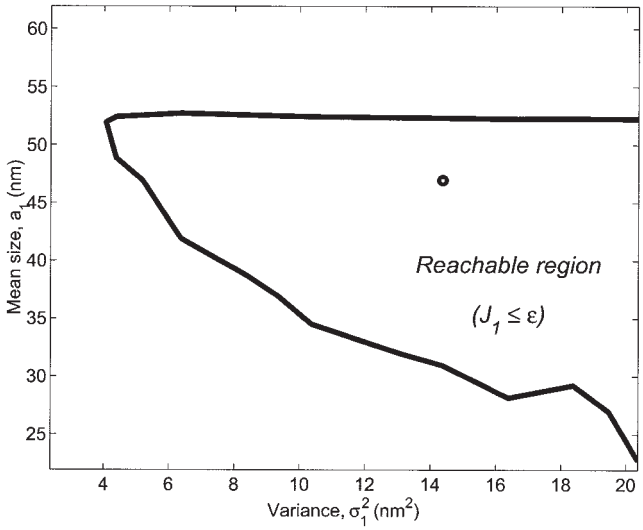

Figure 4. Map of reachable region for the nominal system with $\varepsilon = 0.05$ (circle denotes the reference PSD).

profiles play a critical role in the reachability of the targeted final PSD. This is a strong nonlinearity that may affect the solution of the recipe optimization problems. Unless mentioned otherwise, $S(t_0)$ will be included in the decision variables in all the cases studied hereafter.

Reachable region for the unimodal PSDs

A set of unimodal final PSDs described by a single Gaussian distribution

$$n(r, p) = k_1 \exp[-(r - a_1)^2/\sigma_1^2] \tag{11}$$

is considered, which renders a two-dimensional map of the reachable region (Figure 4) in the parameter space. All the PSD candidates are chosen around one reference PSD, which is characterized by $k_1 = 1.558$, $a_1 = 46.94$ nm, and $\sigma_1 = 14.37$ nm^2. The reference PSD is known to be well reachable with a standardized residual $J_1 = 9.51 \times 10^{-4}$. The equality constraint on solid concentration at the terminal time is used to determine the amplitudes, k_1, of all the candidate PSDs, which are mapped in Figure 3. Given the current ε-specification as 0.05, the resulting reachable region is shown in Figure 4, which corresponds to all the achievable final products under the admissible operating conditions.

Validation of the Current Control Vector Parameterization (CVP). As indicated in the definition of ε-reachability, inaccurate control vector parameterization is one cause of difficulty in assessing reachability. Although a large value of ε could minimize the difficulty, this comes at the expense of less-precise PSD characterization. It is preferred to minimize the variance caused by improper control vector parameterization. To examine the impact of control vector parameterization, the previous reachability analysis is re-evaluated for the nominal system based on a coarser CVP. In detail, each input profile is discretized using five equally spaced heaviside functions, with each piecewise constant control action lasting 20 min.

As seen in Figure 5, the results from the five-element parameterization approach those from the ten-element parameterization. In other words, the previous choice of control vector parameterization is already close to the most efficient solution. In addition, the differences in the standardized residual, J_1, along the boundary of the reachable region (Table 1) show that all the variances caused by the CVP are not only smaller than the specified ε but also at the same level, validating the particular selection of ε.

Dominant Factor for the Reachable Region. As seen in Figure 4, there are drastic changes in the reachability character around both large and small values of a_1. The following discussion will connect these results to both sensitivity studies and kinetic analysis.

An analysis of a representative case (corresponding to $a_1 = 56.94$ nm and $\sigma_1^2 = 12.37$ nm) shows that, for this unreachable PSD, a high $S(t_0) = 1.77 \times 10^{-3}$ mol (see Table 2) along with

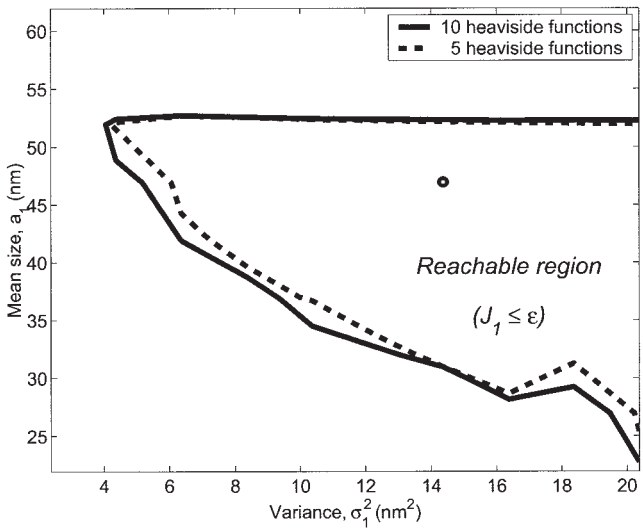

Figure 5. Effort of different control vector parameterization on the reachable region (circle denotes the reference PSD).

Table 1. Differences in J_1 along the Boundary of Current Reachable Region Using Different CVPs

Sample Index	$PSD_{4,5}$	$PSD_{4,6}$	$PSD_{7,10}$	$PSD_{3,7}$	$PSD_{3,9}$	$PSD_{2,10}$
ΔJ_1	1.07×10^{-2}	5.60×10^{-3}	2.00×10^{-2}	2.00×10^{-4}	1.00×10^{-2}	1.25×10^{-2}

later surfactant input were applied to start the micellar nucleation as early as possible while avoiding the undesired secondary mode. The optimized recipe could achieve only the small-size mode of the desired distribution, which kinetic analysis suggests is attributed to the limited particle growth rate.

To validate this hypothesis, the recipe optimization is recomputed with the value of the propagation rate constant k_p (Eq. 5) doubled. As a result, the volumetric particle growth rate will also double, given sufficient monomer within the reactor. The solution of the new recipe optimization problem shows that the previously unreachable PSD is now reachable. Similar sensitivity studies have been conducted for a value of k_p equal to 1/2 the original value. All of these results suggest that the particle growth rate is the dominant factor for reachability, which can be used to explain the boundary around the large a_1 and part of the small a_1. In other words, the reachable region, and the achievable end-point properties can be significantly broadened by manipulating the particle growth rate. One possibility to realize this is through nonisothermal operation of the semibatch reactor, as suggested by Meadows et al.[22] Another potentially easier way is to manipulate the monomer concentration in the reactor.[7] However, the latter operation might undermine the assumptions implicit in the current "zero–one" model.

Effect of a flexible batch time t_f

In addition to manipulating the reactor temperature and monomer concentration, the batch time t_f can also be used to regulate the final PSD. This may become necessary in the presence of disturbances or mismatch in the initial charge. Here, the reachable region of the final PSD is investigated for different batch times $t_f = 2$, 2.5, and 3 h, respectively. Specifically, new decision variables are introduced to the control vector parameterization for the new recipe optimization problems as the batch time is extended. Meanwhile, the reactant feed flow rates remains zero for the last 20 min of reaction, as done in the previous formulation.

The reachability analysis was conducted for styrene system in the presence of the following parametric mismatches:

- +50% mismatch in Langmuir adsorption constants a_s and b_s of the surfactant partition model given by

$$S = S_{ad} + [S]_w v_w$$

$$S_{ad} = \frac{S_{par} + 3v_d/r_d}{a_s N_A} \frac{b_s[S]_w}{1 + b_s[S]_w} \tag{12}$$

- +25% mismatch in critical micelle concentration ($[S_{CMC}]$), which plays a key role in determining the micelle concentration, which in turn determines the micellar nucleation rate

$$[Micelle] = \frac{\ln(e^{10^4([S]_w - [S]_{CMC})} + 1)}{10^4 n_{agg}} \tag{13}$$

In the case of +25% mismatch in the *CMC*, the resulting reachability maps (Figure 6) reveal that the reachable region moves to the area of large particle size as the batch time is extended. This is consistent with the longer evolution of particle nucleation and growth. It is also observed that the reachable region actually is reduced for the mode of small size particles, which could be attributed to two factors. First, because of the constrained surfactant supply during the last 20 min of reaction, the current system has limitations on the achievable small size particles. Second, to generate a mode of small size particles under an extended batch time, the particle nucleation has to be significantly delayed in time. From the perspective of reachability analysis, the system is losing the manipulating capability from the initial charge of reagents (such as surfactant), which could have helped generate the desired final PSD. Clearly, by including t_f as a manipulated variable, the reachable region will be significantly extended along the direction of large mean size (a_1), which will cover each of the above reachable regions obtained with fixed batch times.

Furthermore, as observed in the reachability maps obtained in the cases of +50% mismatches in a_s and b_s, respectively (that is, Figures 7 and 8), the extensions of the front of reachable PSD on large particle mode, Δa_1, are almost identical. This extension is comparatively independent of the model mismatches introduced here. In the next section, quantitative criteria will be developed for the exact value of the extension along the direction of mean size (that is, the Δa_1 in Figure 6). The information would provide guidance when using t_f as a manipulated variable for the in-batch control design.

Quantitative Criterion for Largest Reachable Size. Because of the excess of monomer in the current reaction system, the volumetric particle growth rate becomes essentially size-independent and thus also time-independent. Given a unimodal distribution specified by $p_0 = \{k_1, a_1, \sigma_1\}$ as the targeted final PSD, $n^0(r)$, and considering that the maximum particle size of $n^0(r)$ is subject to a limited particle growth rate, an upper bound for the mean size, a_1, can be determined from the batch time t_f.

Table 2. Sensitivity Study of Doubled k_p

	$\sigma_1 = 12.37$	J_1	$S(t_0)$	Reachable
$a_1 = 56.9$ nm	$k_p = 2.6 \times 10^2$ dm^3 mol^{-1} s^{-1}	0.339	1.8×10^{-3}	No
	$k_p = 5.2 \times 10^2$ dm^3 mol^{-1} s^{-1}	0.0009	6.5×10^{-5}	Yes
$a_1 = 61.9$ nm	$k_p = 2.6 \times 10^2$ dm^3 mol^{-1} s^{-1}	0.838	1.3×10^{-3}	No
	$k_p = 5.2 \times 10^2$ dm^3 mol^{-1} s^{-1}	0.0096	1.6×10^{-5}	Yes

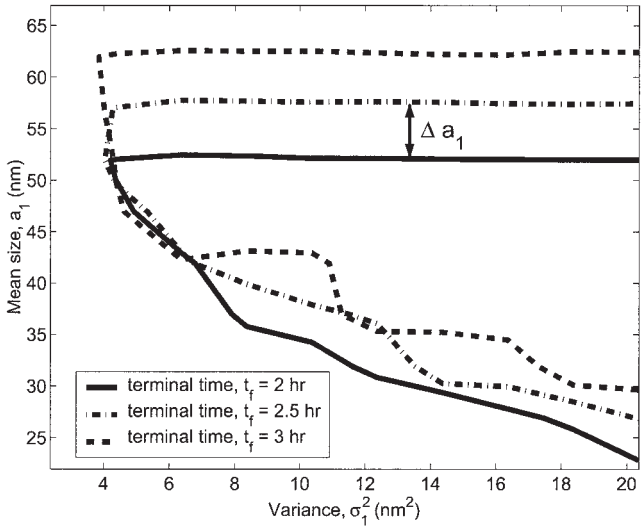

Figure 6. Influence of the batch time t_f on the reachable regions in case of +25% mismatch in $[S_{CMC}]$.

As a first step, a secondary unimodal PSD, $n^1(r)$, is constructed with the largest decrease in maximum particle size while still maintaining the deviation from $n^0(r)$ within specified tolerance ε. Then a specified point in the unimodal distribution needs to be determined as the reference point. The detailed derivation is given as follows:

(1) Given a unimodal distribution, $\acute{n}(r)$, specified by $p_1 = \{\bar{k}_1, \bar{a}_1, \bar{\sigma}_1\}$, its maximum particle size is represented by $\bar{a}_1 + \alpha\bar{\sigma}_1$. The parameter α (>0) is determined by the tolerance β (>0) and the following constraint

$$\int_{\bar{a}_1+\alpha\bar{\sigma}_1}^{\infty} [\acute{n}(r)]^2 dr = \beta \int_{-\infty}^{\infty} [\acute{n}(r)]^2 dr \tag{14}$$

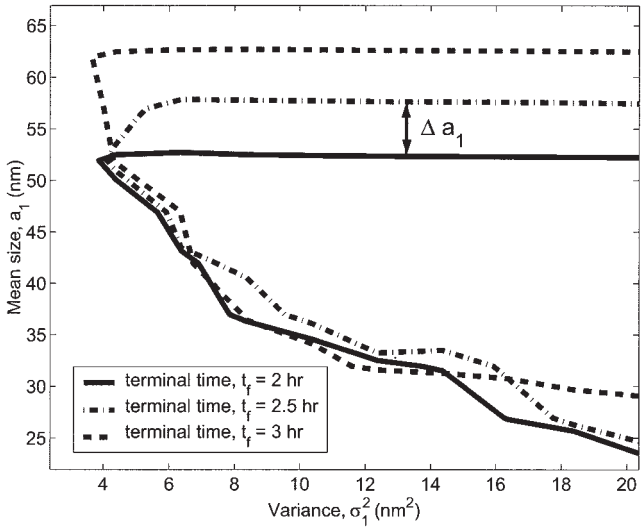

Figure 7. Influence of the batch time t_f on the reachable regions in case of +50% mismatch in a_s.

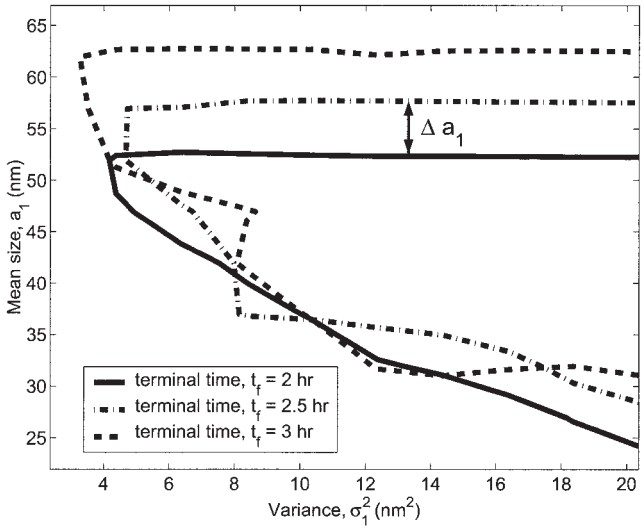

Figure 8. Influence of the batch time t_f on the reachable regions in case of +50% mismatch in b_s.

Clearly, α is independent of p_1 so that it can be solved in advance from a standard normal distribution $\acute{n}(r) = e^{-r^2}$.

(2) Given the threshold value ε, parameters of the secondary distribution $n^1(r) = \bar{k}_1 \exp[-(r - \bar{a}_1)^2/\bar{\sigma}_1^2]$, $p_1 = \{\bar{k}_1, \bar{a}_1, \bar{\sigma}_1\}$ are solved by the following NLP

$$\min_{p_1} \bar{a}_1 + \alpha\bar{\sigma}_1$$

$$\text{s.t.} \int_{-\infty}^{\infty} [n^0(r) - n^1(r)]^2 dr \le \varepsilon \int_{-\infty}^{\infty} [n^0(r)]^2 dr \tag{15}$$

Similarly, $c_0 = \bar{k}_1/k_1$, $c_1 = (a_1 - \bar{a}_1)/\sigma_1$, and $c_2 = \bar{\sigma}_1/\sigma_1$ are constants determined only by the threshold value ε, and also can be solved in advance.

(3) The maximum particle size of the secondary distribution $n^1(r)$

$$r^* = a_1 + (\alpha c_2 - c_1)\sigma_1 \tag{16}$$

is constrained by the limited particle growth rate for the ab initio system, and is subject to

$$r^* \le \left[r_{nuc}^3 + \frac{3k_p C_p w_m}{4\pi\rho_P N_A} (t_f - t_0) \right]^{1/3} \tag{17}$$

Criterion 1. *Assuming a surplus of monomer in the reactor during the batch, it is impossible to reach a unimodal final PSD at time t_f with the mean size*

$$a_1 > \left[r_{nuc}^3 + \frac{3k_p C_p w_m}{4\pi\rho_P N_A} (t_f - t_0) \right]^{1/3} - (\alpha c_2 - c_1)\sigma_1 \tag{18}$$

Accordingly, a quantitative estimate can be calculated for the extension of the front of reachable PSDs on the large particle mode, Δa_1

Table 3. Comparison of Predicted and Measured Δa_1 in Case of +25% Mismatch in $[S_{CMC}]$

Δa_1 (nm) (with t_f extended)	σ_1 (nm^2)								Δa_1 (nm)	
	6.37	8.37	10.37	12.37	14.37	16.37	18.37	20.37	Average	Predicted
From 120 to 150 min	5.284	5.311	5.431	5.482	5.488	5.396	5.393	5.467	5.407	5.822
From 150 to 180 min	4.812	4.825	4.945	4.730	4.626	4.727	5.061	4.977	4.838	5.091

$$\Delta a_1 = \left[r_{nuc}^3 + \frac{3k_pC_pw_m}{4\pi\rho_PN_A}(t_{f,new} - t_0) \right]^{1/3} - \left[r_{nuc}^3 + \frac{3k_pC_pw_m}{4\pi\rho_PN_A}(t_f - t_0) \right]^{1/3} \quad (19)$$

The quantitative estimates of Δa_1 for different t_f values are validated for the styrene system by the reachable region information obtained in the previous section (Figures 6–8). As seen in Table 3 for the case of +25% mismatch in $[S_{CMC}]$, the predicted Δa_1 is consistent with the simulated data.

Results for the Perturbed System

In the previous section, the reachable unimodal PSDs for a known zero–one system have been analyzed. However, in many practical applications, this map of achievable products could be dramatically changed because of inevitable disturbances from the upstream supply, as well as the uncertainties and unmodeled dynamics in the original system. From an industrial perspective, it is even more important to understand how the reachable region will change in response to perturbations in the key reaction kinetics.

Sensitivities to parametric mismatches

A sensitivity study of the reachable region was performed for the parametric mismatches indicated in Eqs. 12 and 13. In addition to their importance in the polymerization mechanisms, these parameters are also among the most difficult to be identified.

The results of the sensitivity analysis are shown in Figure 9,

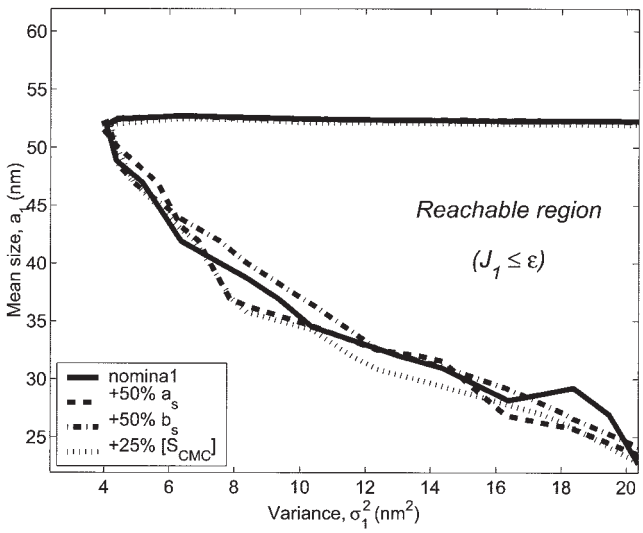

Figure 9. Sensitivity of the reachable region to key parametric mismatches.

compared with the nominal reachable region bounded by the solid line (that is, the shadowed area). Despite the presence of significant parametric mismatch, the reachable final PSDs do not show dramatic changes in the shape of the entire reachable region. In effect, the current system shows a certain level of robustness in the achievable end-point products, as long as accurate information about the current model mismatch had been provided at the start of the reaction. However, given the infrequent, unreliable on-line measurements of PSD as well as the limitation on the earliest sampling time, the above assumption is unrealistic in practice.

Reachability of midcourse correction

Midcourse correction is a control policy frequently applied to semibatch processes with irregular measurements and excessive measurement delays.[6,23] The reactor is charged and operated based on a standard recipe until a specified moment, at which time a first latex sample is collected and lab analyses are performed. Once the intermediate PSD information is available, a model-based estimator is used to identify the disturbances and predict the final PSD.

- If the prediction falls within a region (specified by ε) around the original target, then no midcourse adjustment is needed.
- Otherwise, the reachability analysis results are used to decide a proper PSD control strategy under the current conditions:
  - —If the original target becomes unreachable (that is, it is impossible to correct the influence of the current disturbance by later inputs), disturbance would be recorded and handled through a batch-to-batch control.
  - —If the PSD remains reachable, the best profiles for the future inputs will be determined by iterative recipe optimization.

However, there is competition between the identification accuracy and capacity of midcourse correction (that is, the midcourse reachability). In practice, one has only a few opportunities to collect intermediate PSD information, whereas a minimal reaction time is needed before the influence of these disturbances become distinguishable. On the other hand, the reachable region will continue to shrink with time, and eventually degenerate into a single point (that is, the actual final PSD produced). Therefore, it is necessary to evaluate the evolution of the reachable region throughout the batch to determine the optimal sampling moments.

The formulation and assessment of the ε-reachability under midcourse correction is identical to the formulation given in Eqs. 6–8, with the exception of the shrinking control horizon, and the assumption of perfect knowledge of the current disturbances and the initial conditions.

Case of +25% Mismatch in $[S_{CMC}]$. The evolution of the reachable region is evaluated every 10 min during the first 40 min of the reaction in the presence of a +25% mismatch in

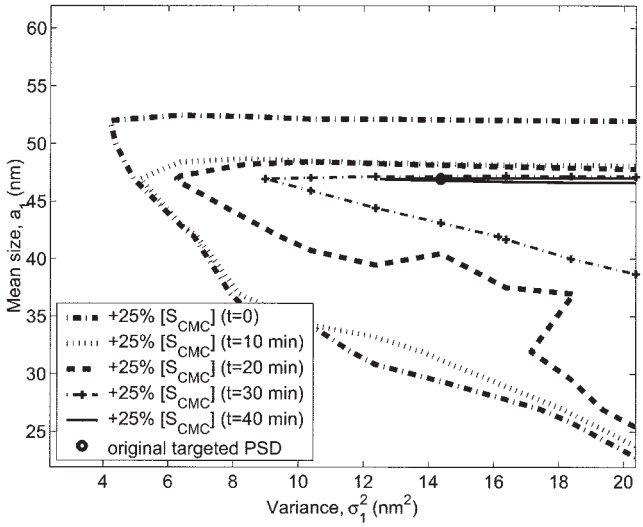

Figure 10. Evolution of the reachable region in case of +25% mismatch in [S_{CMC}].

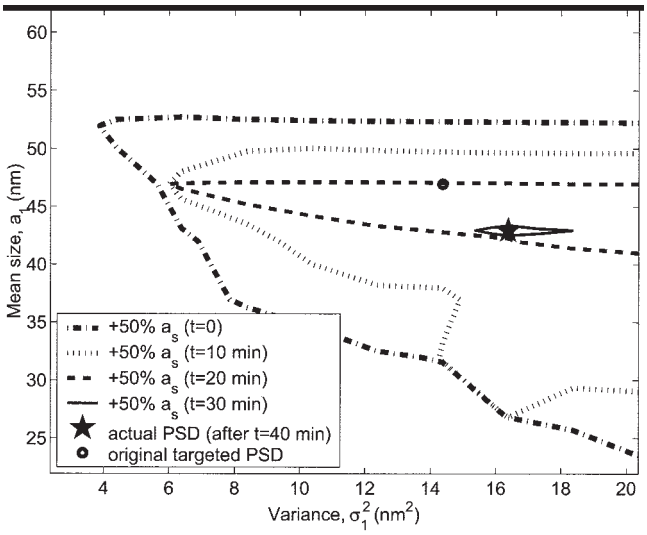

Figure 11. Evolution of the reachable region in case of +50% mismatch in a_s.

[S_{CMC}] (the designation "+" indicates that the parameter is 25% above the true value). To assess the reachable region, the exact model mismatch is assumed to be identified immediately after the sampling moment. The following observations are revealed from an analysis of the reachability maps (Figure 10):

- During the early stage of the reaction (that is, the first 10 min), loss of the reachable region is primarily associated with the mode of large size particles because the initial reagent charge could no longer be used to achieve the desired primary micellar nucleation.
- Thereafter the main reduction of the reachable region is in the mode of small size particles because most of the surfactant has been consumed by the previous nucleation event.
- Shortly after $t = 40$ min, the original targeted PSD (indicated by the circle) will fall outside the reachable region. That is, the reachable region declines so dramatically that if no corrective action has been taken before $t = 40$ min, the original targeted PSD can never be reached after that moment.

As a result, a reliable PSD measurement is required before $t = 40$ min to achieve effective control of the final PSD.

Case of +50% Mismatch in a_s. Similar reachability analysis was conducted for the perturbed system with +50% mismatch in a_s (Figure 11). Compared with the previous perturbed case on [S_{CMC}], the reachable region dissipates even more quickly. Shortly after $t = 20$ min, the original targeted PSD falls outside the reachable region. There is almost no effect of control action after $t = 30$ min. Because of the large value in actual a_s, more surfactant is needed to generate the originally desired particle nucleation profile. However, given the upper-bound constraints on the surfactant feed rate, the later surfactant feed after $t = 30$ min could not make up the demanded surfactant concentration.

Considering the limitation on the earliest sampling time and the inevitable measurement delay, the intermediate PSD information required in this case might be too difficult to attain for on-line control. If such variation in a_s is realistic in typical operations, the nominal recipe should be carefully revised to make the final PSD controllable.

Case of +50% Mismatch in b_s. Considering the evolution of the reachable region in presence of a +50% mismatch in b_s (Figure 12), the influence of this particular mismatch is moderate. Similar to the [S_{CMC}] case, one can observe:

- The reachable region is mainly affected by the mode of large size particles during the early stage of the reaction.
- Even after $t = 40$ min, the original targeted final PSD remains at the center of the reachable region.

This suggests that in-batch control would be facilitated by identification of a perturbation and subsequent reoptimization of the control action. On the other hand, the insensitivity of the system to the model mismatch might cause some difficulties in identifying the actual value of b_s.

In summary, considering the limited measurement available from the emulsion process, the reachability analysis plays an essential role in determining the proper on-line control strategy.

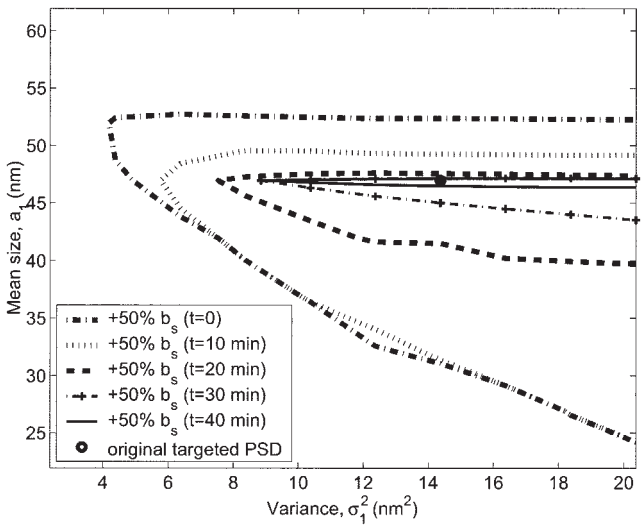

Figure 12. Evolution of the reachable region in case of +50% mismatch in b_s.

Conclusion

A systematic approach has been proposed for reachability analysis of general particulate systems described by population balance equations. The application to a semibatch styrene emulsion polymerization process illustrates its efficiency in determining the on-line control strategy and critical operating conditions.

The discussion highlights the importance of proper initial reaction conditions as well as the nonlinearity inherent in the recipe optimization problems. For the reachability of unimodal PSDs, the limiting factors of reaction temperature and batch time are identified, along with a quantitative criterion for the reachable region. The study also suggests a certain level of robustness in the reachable region against uncertainties in the surfactant partition parameters and the $[S_{CMC}]$ values. The reachability studies in the case of midcourse correction have highlighted the importance of early PSD measurements, and proper early corrective action.

Acknowledgments

The authors gratefully acknowledge the funding from Air Products and Chemicals Inc. In addition, the authors acknowledge the active collaborations with Dr. Cajee Cordeiro and the polymer group at Air Products and Chemicals.

Notation

a_1, a_i, $\bar{a}_1$ = mean sizes of the modes in final PSD, nm
a_s, b_s = Langmuir adsorption constants, dm^2 and dm^3/mol
c_0, c_1, c_2 = constants used in determining Δa_1
C_p = monomer concentration in polymer particles
$[E]$ = concentration of uncharged monomer radicals in the aqueous phase
$G(r)$ = volumetric particle growth rate
$[IM_i]$ = concentration of polymer radical with i monomer units
J_1 = objective function in recipe optimization
$k_0(r)$ = radical exit rate from the particle
k_1, k_i, $\bar{k}_1$ = amplitudes of the modes in final PSD
$k_{e,E}$ = rate coefficient for entry of monomer radicals into particles
$k_{em,i}$ = rate coefficient for micellar nucleation by polymer radicals
k_p = propagation rate constant, $dm^3\ mol^{-1}\ s^{-1}$
k_{pe} = propagation rate coefficient for monomer radicals in particles
k_{tr} = rate coefficient for chain transfer to monomer within polymer particles, $dm^3\ mol^{-1}\ s^{-1}$
$[Micelle]$ = micelle concentration in the aqueous phase
n_{agg} = micelle nucleation constant
$n(r, t)$ = number density of particle size r per unit volume at moment t
$n_0(r)$ = number density of particle containing zero radical
$n_1(r)$ = number density of particle containing one radical
$n_1^m(r)$ = number density of particle containing one monomer radical
$n_1^p(r)$ = number density of particle containing one polymer radical
n_{scale} = standardization factor for ε-reachability
$n^{model}(r)$ = final PSD predicted by current model
$n^{target}(r)$ = targeted final PSD
N_A = Avogadro's number
p, p_0, p^1 = parameter vectors to characterize the final PSD
r = particle size in radius, m
r_d = radius of monomer droplets, m
r_{nuc} = particle size that nucleation occurs, m
S = surfactant concentration, mol
$[S_{ad}]$ = moles of surfactant adsorbed on the surface of particles and monomer droplets
$[S_{CMC}]$ = critical micelle concentration
$[S_w]$ = free surfactant concentration
t_0 = initial time
t_f = terminal/batch time
v_d = volume of monomer droplets
v_w = volume of aqueous phase
w_m = molecular weight of monomer
$x(t)$ = state vector at moment t

Greek letters

α, β = parameter and tolerance used in determining Δa_1
$\delta(r)$ = Delta function denoting the boundary condition from particle nucleation
ε = threshold value for approximated reachability
$\rho(r)$ = overall radical entry rate into particles
ρ_{init} = entry rate of initiator derived polymer radicals only
ρ_P = density of polymer
σ_1, σ_i, $\bar{\sigma}_1$ = variances of the modes in final PSD, nm^2

Literature Cited

1. Gilbert RG. *Emulsion Polymerization: A Mechanistic Approach.* San Diego, CA: Academic Press; 1995.
2. Immanuel CD, Cordeiro CF, Sundaram S, Meadows ES, Crowley TJ, Doyle FJ III. Modeling of particle size distribution in emulsion copolymerization: Comparison with experimental data and parametric sensitivity studies. *Computers and Chemical Engineering*. 2002;26:1133-1152.
3. Congalidis JP, Richards JR. Process control of polymerization reactors: An industrial perspective. *Polymer Reaction Engineering*. 1998;6:71-111.
4. Doyle FJ III, Soroush M, Cordeiro CF. Control of product quality in polymerization processes. In: Rawlings JB, Ogunnaike BA, Eaton JW, eds. *AIChE Symposium Series: Chemical Process Control-VI*; 2001:290-306.
5. Daoutidis P, Henson MA. Dynamics and control of cell populations in continuous bioreactors. In: Rawlings JB, Ogunnaike BA, Eaton JW, eds. *AIChE Symposium Series: Chemical Process Control-VI*; 2001:274-289.
6. Flores-Cerrillo J, MacGregor JF. Control of particle size distributions in emulsion semibatch polymerization using mid-course correction policies. *Industrial and Engineering Chemistry Research*. 2002;41:1805-1814.
7. Liotta V, Georgakis C, El-Aasser MS. Controllability issues concerning particle size in emulsion polymerization. In: *IFAC Symposium on Dynamics and Control of Process Systems-IV*. Helsingør, Denmark; 1995;299-304.
8. Ma DL, Tafti DK, Braatz RD. Optimal control and simulation of multidimensional crystallization processes. *Computers and Chemical Engineering*. 2002;26:1103-1116.
9. Semino D, Ray WH. Control of systems described by population balance equations—I. Controllability analysis. *Chemical Engineering Science*. 1995;50:1805-1824.
10. Semino D, Ray WH. Control of systems described by population balance equations—II. Emulsion polymerization with constrained control action. *Chemical Engineering Science*. 1995;50:1825-1839.
11. Ramkrishna D. *Population Balances: Theory and Applications to Particulate Systems in Engineering*. San Diego, CA: Academic Press; 2000.
12. Braatz RD, Hasebe S. Particle size and shape control in crystallization processes. In: Rawlings JB, Ogunnaike BA, Eaton JW, eds. *AIChE Symposium Series: Chemical Process Control-VI*; 2001:307-327.
13. Ramkrishna D. The status of population balances. *Reviews in Chemical Engineering*. 1985;3:49-95.
14. Rawlings JB, Miller SM, Witkowski WR. Model identification and control of solution crystallization processes: A review. *Industrial and Engineering Chemistry Research*. 1993;32:1275-1296.
15. Lions JL. Exact controllability, stabilization and perturbations for distributed systems. *SIAM Review*. 1988;30:1-68.
16. Russell DL. Controllability and stabilizability theory for linear partial differential equations: Recent progress and open questions. *SIAM Review*. 1978;20:639-739.
17. Crowley TJ, Meadows ES, Kostoulas E, Doyle FJ III. Control of particle size distribution in semibatch emulsion polymerization by surfactant addition. *Journal of Process Control*. 2000;10:419-432.
18. Coen EM, Gilbert RG, Morrison BR, Leube H, Peach, S. Modeling particle size distributions and secondary particle formation in emulsion polymerization. *Polymer*. 1998;39:7099-7112.

19. Immanuel CD, Cordeiro CF, Sundaram SS, Doyle FJ III. Particle size distribution model for emulsion copolymerization under steric stabilization. *AIChE Journal*. 2002;49:1392-1404.
20. Stengel RF. *Stochastic Optimal Control: Theory and Application*. New York, NY: Wiley; 1986.
21. Zhou JL, Tits AL, Lawrence CT. User's guide for FFSQP Version 3.7: A Fortran code for solving optimization programs, possibly minimax, with general inequality constraints and linear equality constraints, generating feasible iterates. *Technical Report SRC-TR-92-107r5*. Institute for Systems Research, University of Maryland, College Park; 1997.
22. Meadows ES, Crowley TJ, Immanuel CD, Doyle FJ III. Nonisothermal modeling and sensitivity studies for batch and semibath emulsion polymerization of styrene. *Industrial and Engineering Chemistry Research*. 2003;42:555-567.
23. Yabuki Y, MacGregor JF. Product quality control in semibatch reactors using midcourse correction policies. *Industrial and Engineering Chemistry Research*. 1997;36:1268-1275.

Manuscript received Aug. 21, 2003, and revision received Mar. 16, 2004.